Journal of Power Sources 183 (2008) 20–25

Contents lists available at ScienceDirect

Journal of Power Sources

journal homepage: www.elsevier.com/locate/jpowsour

Novel copper-based anodes for solid oxide fuel cells with samaria-doped ceria electrolyte

A.C. Tavares[a,*], B.L. Kuzin[b], S.M. Beresnev[b], N.M. Bogdanovich[b], E.Kh. Kurumchin[b], Y.A. Dubitsky[a], A. Zaopo[a]

[a] Pirelli Labs, Viale Sarca 222, 20126 Milano, Italy
[b] Institute of High-Temperature Electrochemistry Ural Division of Russian Academy of Sciences, S. Kovalevskoj 22, 620219 Yekaterinburg, Russia

ARTICLE INFO

Article history:
Received 13 March 2008
Received in revised form 1 May 2008
Accepted 1 May 2008
Available online 7 May 2008

Keywords:
Solid oxide fuel cell
Cu and samaria-doped ceria anode
Ceramic technology
Ni and CeO_2-dispersed phases
Hydrogen
Methane

ABSTRACT

A novel copper-based anode for low-temperature solid oxide fuel cells was prepared through the conventional ceramic technology and using CuO and SDC ($Ce_{0.8}Sm_{0.2}O_{1.9}$) powders with controlled particle size. The new Cu–SDC anode also contained highly dispersed CeO_2 and Ni particles to increase its surface area and fuel cell performance. The specific surface area of the Cu–SDC bare anode, CeO_2 and Ni-dispersed phases were estimated to be 1.53, 39.4 and 86.4 $m^2 g^{-1}$, respectively. Solid oxide fuel cells having the new anode were tested for both humid hydrogen and methane. Power densities of ca. 250 mW cm^{-2} were achieved in H_2 at 600 °C and in CH_4 700 °C, even if the SDC–electrolyte supporting membrane was 250-μm thick. Short term stability tests (maximum 64 h) showed an initial impairment, but not dramatic, of the new anode performance and the formation of carbon deposits. The addition of MoO_x to the new anode did not prevent the formation of carbon deposits.

1. Introduction

Solid oxide fuel cells (SOFCs) convert chemical energy into electrical energy with high efficiency and low emission of pollutants. Although the introduction of a "green energy" might seem an attractive scenario, its implementation is beset with economical and technical difficulties. Today's SOFC technology is based on Ni–YSZ (YSZ = Y_2O_3–ZrO_2) anodes which operate very efficiently with pre-reformed natural gas or with hydrogen at high temperatures. However, for some applications such as distribution of electrical energy, natural gas is an attractive fuel because of the existing infrastructure and widespread availability. Methane, major component of natural gas, can be externally reformed producing H_2 and CO-rich gas, which is then used to operate the fuel cell. Methane can be also internally reformed at the Ni–YSZ anode of SOFCs operating at high temperatures, but a high steam-to-methane ratio is required to prevent the methane cracking reaction. Methane cracking produces carbon deposits with serious losses of the Ni–YSZ anode performance [1–3]. In this scenario, fuel cell operation with direct utilisation of hydrocarbon fuel, often referred as electrochemical oxidation of hydrocarbons, and without the addition of a considerable amount of water would contribute to system simplicity and reduction of the overall cost.

Different strategies have been pursued to develop new anode materials and new anode configurations able to operate directly with hydrocarbons, especially with methane. One approach consists in replacing nickel by copper in the cermet anode, because copper does not catalyse the cracking process. Another approach consists in lowering the fuel cell operation temperature since the rate of carbon formation decreases with temperature [4]. Another advantage of low-temperature (<800 °C) operation is the use of stainless steel in the construction of house holdings and a further cost reduction.

Gorte and co-workers have carried out an important work on the development of Cu–cermet anodes for SOFCs operating with hydrocarbon fuels. Their efforts have been focused on Cu/CeO_2/YSZ and Cu/CeO_2/SDC anodes for H_2, methane and butane oxidation [3,5–7]. Their anodes are generally obtained by impregnating of a porous thick layer of YSZ or SDC materials with aqueous solutions of $Cu(NO_3)_2$ and $Ce(NO_3)_3$. Ceria (CeO_2), a catalytic material for hydrocarbon oxidation, is used to enhance the anode performance. The reported power densities depend on the fuel type, electrodes and electrolyte composition, and electrolyte thickness. For example, this group achieved 0.3 W cm^{-2} in dry

* Corresponding author. Present address: Institut National de la Recherche Scientifique – Énergie, Matériaux et Télécommunications, 1650 Boulevard Lionel Boulet, Varennes, Québec, Canada J3X 1S2. Tel.: +1 450 929 8147; fax: +1 450 929 8102.
E-mail address: ana.tavares@emt.inrs.ca (A.C. Tavares).

0378-7753/$ – see front matter © 2008 Elsevier B.V. All rights reserved.
doi:10.1016/j.jpowsour.2008.05.003

hydrogen, 0.12 W cm^{-2} in dry butane and 0.09 W cm^{-2} in dry methane with a Cu (20 wt%)–CeO_2–YSZ (400 μm)/YSZ electrolyte (60 μm)/(50/50 wt%) YSZ–SLM fuel cell operating at 700 °C [6]. In another work, the same group reported a maximum power density of 40 mW cm^{-2} for Cu (40 wt%)–CeO_2–YSZ anode/YSZ electrolyte (230 μm)/(50/50 wt%) YSZ–Sr–$LaMnO_3$ operating in dry methane at 700 °C [3].

Copper and copper oxides have a low melting point, and copper particles tend to sinter and to form agglomerates during fuel cell operation. Joerger et al. [8] investigated Cu–CGO (copper–gadolinium-doped ceria) anodes prepared using two different methods: direct precipitation of $Cu(OH)_2$ onto the submicrometer CGO powder and ball milling of CuO with coarse CGO. Heterogeneous microstructures with large agglomerates of copper were obtained, and the copper grains tended to coarse during fuel cell operation. Single SOFC cell measurements were done in methane diluted with nitrogen; at 800 °C the OCV was only 0.5 V and the maximum power output was 10 mW cm^{-2}. The authors attribute this limited performance to the thermal decomposition of methane with carbon deposition and/or to the ongoing copper sintering. In a recent paper [7] Gorte and co-workers showed that the addition of Cu to the porous YSZ layer via impregnation of aqueous copper nitrate solutions results in an inhomogeneous distribution of the copper. The addition of urea to the nitrate solution during the anode preparation improves the copper distribution throughout the porous YSZ anode, and the resulting anodes exhibited a good performance in humidified hydrogen at 700 °C. However, annealing at higher temperatures (800 and 900 °C) leads to the agglomeration of Cu layer and the formation of isolated copper particles and performance degradation.

The performance of copper-based anodes of SOFCs fed directly with methane and within 600–800 °C temperature range still needs to be improved. Issues on the development of Cu-based anodes include the uniform distribution of copper particles throughout the anodes, the sintering of copper particles and the development of a simple cell fabrication process that assures reproducibility and scale up.

In this paper we report the preparation and the electrochemical characterisation of a Cu–SDC anode prepared using the conventional ceramic technology from CuO and SDC powders, and further activated with catalytically active particles of CeO_2 and Ni. The new anode was tested in both humidified (3 vol%) hydrogen and methane, between 500 and 700 °C. Molybdenum oxide was also added to the new anode in an attempt to mitigate carbon deposition and the consequent anode deactivation.

2. Experimental

2.1. Materials and anode fabrication

The new Cu–SDC anode consists of a porous Cu–SDC (60–40 wt%) based cermet with catalytic particles finely dispersed through it. The Ni–YSZ conventional ceramic technology [9] was used to prepare the Cu–SDC base cermet. The preparation process, optimised for this specific cermet composition, included the milling of CuO and SDC starting powders to control the particle size and surface area, their intensive mixing, and an intermediary grinding and thermal treatments before the final sintering. The detailed cermet preparation procedure can be found elsewhere [10], however a brief description is next presented.

2.1.1. $Ce_{0.8}Sm_{0.2}O_{1.9}$ (SDC) electrolyte materials

The SDC powder used for anode fabrication was prepared by solid state reaction using CeO_2 and Sm_2O_3 (quality Ce–L and Sm–L, respectively, >99.9% purity fabricated at OAO "Uralredmet") [11]. The conductivity measured in air at 650 °C was 0.0313 S cm^{-1} and the activation energy—57.4 kJ mol^{-1}. The baked SDC pellets were broken in a porcelain mortar and wet-ground using a planetary mill with jasper balls and isopropyl alcohol to a final average particle size d = 3 μm and S = 1.9 m^2 g^{-1} surface area. The SDC powders used for the membrane fabrication were prepared by co-precipitation of hydroxides from a stoichiometric nitrate solution (purity >99.5%, Novosibirsk Plant of Rare Metals). The hydroxides were compacted into pellets with 12 mm diameter under a pressure of 500 MPa, and then sintered in air at 1300 °C for 2 h. The structure and phase purity were determined by X-ray diffraction. The conductivity in air at 650 °C was 0.0247 S cm^{-1} and the activation energy—69.4 kJ mol^{-1}. Electrolyte membranes 250 and 560 μm thick were used in the fuel cell fabrication.

2.1.2. Cu–SDC anode preparation

CuO ("analytically pure" grade, >99.5%; ground to a final average particle size of 3.4 μm and 0.9 m^2 g^{-1} surface area) and SDC (S = 1.9 m^2 g^{-1} surface area) powders were mixed in a planetary mill with jasper balls with the aid of isopropyl alcohol. After solvent removal the powder mixture was blended with polyvinyl alcohol, pelletized under a pressure of 30 MPa, and heat-treated at 800 °C in air for 1.5 h. The CuO–SDC pellet was milled again until a final surface area S = 3.3 m^2 g^{-1} and average particle size d = 3.3 μm. A CuO–SDC slurry was prepared from this fine powder mixture and a binder, and brushed onto several SDC electrolyte membranes. The CuO–SDC layers were fired in air at 1050 °C. After fabrication of the three-electrode cell the anode was reduced in humid hydrogen at 500 °C (see below). Each Cu–SDC anode had a thickness of 30–40 μm and geometric area of nearly 0.3 cm^2.

The Cu–SDC anodes were further impregnated with aqueous solutions of $Ce(NO_3)_3$ (firstly) and $Ni(NO_3)_2$ (secondly), followed by thermal annealing at 500 °C and reduction in humid H_2. Some anodes were also impregnated with a solution of $(NH_4)_6Mo_7O_{24}{\cdot}4H_2O$ (thirdly). The solutions concentration was 140 g/100 ml for $Ce(NO_3)_3$, 167.5 g/100 ml for $Ni(NO_3)_2$ and 4.14 g/100 ml for $(NH_4)_6Mo_7O_{24}$. The quantity of material deposited after each step was estimated by weight difference and corresponded to 4.8 mg of CeO_2 (9 wt%), 1.2 mg Ni (2 wt%) and 0.50 mg MoO_x (1.4 wt%). This method, well known in literature, is an effective way to promote the electrochemical reactions and to improve the anodes [12,13].

2.2. Morphological characterisation of the new Cu–SDC anode

The morphology and relative phase distribution of the new Cu–SDC anode were assessed with a scanning electron microscope (JSM-5900LV) and EDX analysis. The specific surface area of the Cu–SDC bare anode and with (CeO_2 + Ni) was determined by the nitrogen BET method using a Sorpty 1750 from Carlo Erba Strumentazione in the following sequence: bare Cu–SDC anode; anode impregnated with CeO_2; anode impregnated with CeO_2 + Ni. It was assumed that the surface area of the underneath anode did not change during each activation step, and the surface area increase after each activation results from the deposition of the highly dispersed catalytic phases CeO_2 and Ni. Ten Cu–SDC bare anodes were deposited over 10 SDC electrolyte plates for a total 31.2 cm^2 apparent surface area; then, the subsequent procedure was adopted:

- reduction of the Cu–SDC bare anodes and determination of their specific surface;
- samples calcination in a Ar + H_2 + H_2O mixture at a temperature of 600 °C for 1 h; weighing;

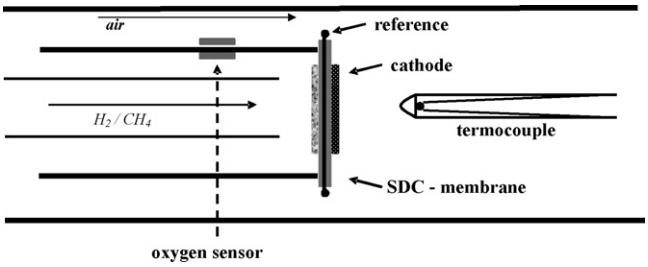

Fig. 1. Diagram of the electrochemical set-up used for fuel cell testing.

- impregnation of the anodes with a $Ce(NO_3)_3$ solution (140 g/100 ml); calcination in a $Ar + H_2 + H_2O$ mixture at a temperature of 600 °C for 1 h; weighing and determination of the specific surface area;
- calcination of the samples in a $Ar + H_2 + H_2O$ mixture at a temperature of 600 °C for 1 h; weighing;
- impregnation of the anodes with a $Ni(NO_3)_3$ solution (168 g/100 ml). Calcination in a $Ar + H_2 + H_2O$ mixture at a temperature of 600 °C for 1 h; weighing and determination of the specific surface area;
- in all the cases the samples were heated and cooled at a rate of 100 °C h^{-1}.

2.3. Fuel cell measurements

A three-electrode measuring cell was used. A diagram of the experimental set-up is shown in Fig. 1. A disk-shaped (diameter 12 mm) sample was pressed under a spring load to the end face of a tube made of a zirconia-based solid electrolyte. The working electrode was the new Cu–SDC anode, while the cathode was made of a fine $Pt + PrO_x$ paste [14]. The reference electrode was arranged in the same way as in [15]. A platinum wire was wrapped round the lateral surface of the SDC disk and fixed with Pt paste. The Pt wire was of 0.1 mm in diameter. To increase the electrochemical activity the reference electrode was impregnated with alcohol solution of $Pr(NO_3)_3$ and heat-treated to decompose the salt to PrO_{2-x}. When the current flows through the fuel cell the voltage differences measured between the polarized electrodes and the reference electrode are $\Delta\varphi_{cr} = \varphi_c - \varphi_r = \eta_c + IR_{cr}$ for the cathode and $\Delta\varphi_{ar} = \varphi_{oc} - (\eta_a + IR_{ar})$ for the anode. Reliability of the reference electrode follows from the facts that (i) in open circuit conditions the voltage between the cathode and reference electrode was not higher then 1 mV; (ii) when a current flows through the cell both cathode and anode ohmic contributions to the total IR drop were close to each other as it should be when the reference electrode is placed in the middle of the side-wall of the SDC disk; (iii) the cathode overvoltage did not depend on the composition of the gas in the anode half-space. The anode faced the inside compartment while the cathode faced the outside one. The external surface of the tube was blown with air, while humid hydrogen or methane (3.5 vol% H_2O) was fed to the anode compartment. The fuels flow rate was 4.8 l h^{-1} for hydrogen and 2.7 l h^{-1} for methane.

The following fuel cells were tested in both humid hydrogen and methane:

Cell I: $(H_2/CH_4 + H_2O)$, Cu–SDC $(CeO_2 + Ni)$/SDC (250 μm)/$Pt + PrO_{2-x}$, air
Cell II: $(H_2/CH_4 + H_2O)$, Cu–SDC $(CeO_2 + Ni)$/SDC (560 μm)/$Pt + PrO_{2-x}$, air
Cell III: $(H_2/CH_4 + H_2O)$, Cu–SDC $(CeO_2 + Ni + MoO_x)$/SDC (560 μm)/$Pt + PrO_{2-x}$, air.

The cell performance and electrodic overvoltage were recorded under stationary conditions (galvanostatic mode) and the ohmic drop was measured by the current interruption method.

3. Results and discussion

3.1. Morphological characterisation

Fig. 2 shows the microstructure (top-view) of two Cu–SDC anodes: (a) bare anode and (b) a Cu–SDC anode impregnated with $CeO_2 + Ni$. Fig. 3 demonstrates the elemental distribution maps for Cu, Ce and Ni over a cross-section of an impregnated Cu–SDC-based anode. The analyzed element is in black. These figures show the typical porous structure of the new anode, and the EDX mappings demonstrate that all elements, including Ni, are distributed rather uniformly over the anode structure. These images confirm that the size of nickel particles is significantly smaller than those of the base Cu–SDC cermet. Also, these pictures clearly show that the new Cu–SDC anode presents a suitable structure for a SOFC electrode: porosity for fuel delivery and products removal, ionic and electronic networks, as well as uniform distribution of the catalytic sites where the fuel conversion takes place.

The conventional ceramic technology presents several advantages especially when commercial powders are used: reproducibil-

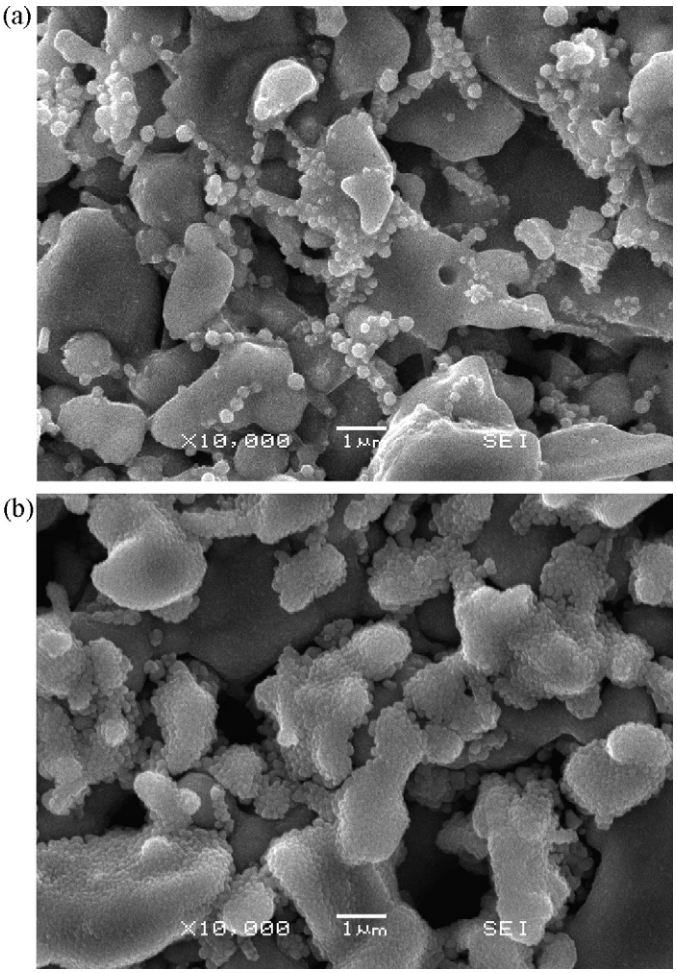

Fig. 2. SEM images (top-view) of (a) Cu–SDC bare anode and (b) impregnated with CeO_2 and Ni highly dispersed phases.

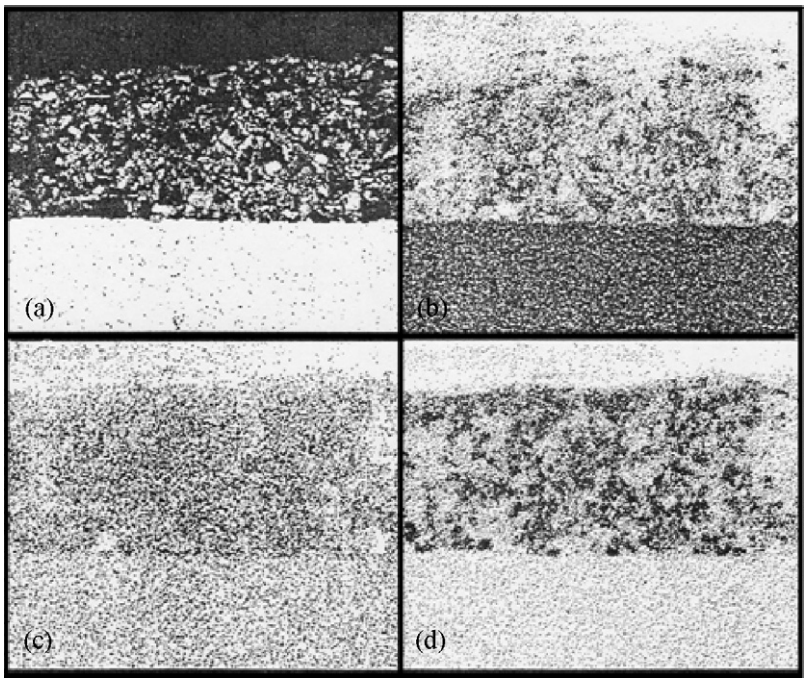

Fig. 3. SEM images and elemental distribution of a cross-section of a Cu–SDC anode impregnated with CeO_2 and Ni highly dispersed phases: (a) back-scattering mode, (b) cerium, (c) nickel, (d) copper; the analysed element is in black.

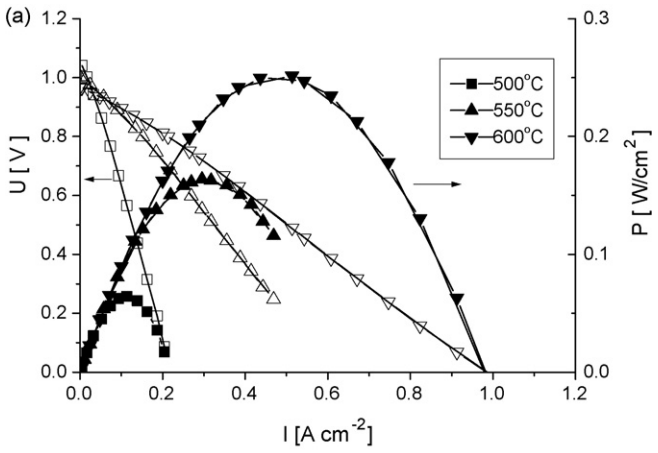

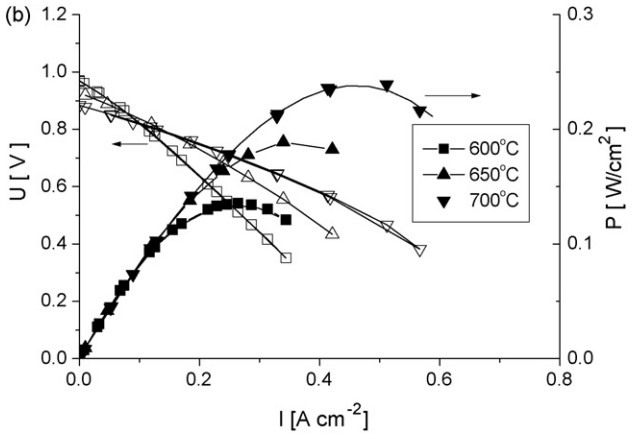

Fig. 4. Cell potential (U) and power density (P) as function of the current density for fuel cell I (Ni–CeO_2)–Cu–SDC/SDC/Pt + PrO_{2-x} in (a) humidified hydrogen/air and (b) humidified methane/air; electrolyte membrane thickness 250 μm.

ity, quality control and cost of the process and raw materials. However it is often difficult to achieve an optimum phase distribution, by this technique. In addition, copper and copper oxides have a low melting point which obliges to special precautions during the preparation of Cu–cermet: our work has shown that an intermediary step of grinding is beneficial to improve the anode structure.

Besides to a proper phase distribution, high surface area is fundamental to accelerate the catalytic reactions. In the ceramic technology high sintering temperatures are used and the resulting anodes have low surface area. The dispersion of finally divided particles of a catalytic material throughout the anode is an effective procedure to increase the anode surface area. We have estimated the specific surface areas of the Cu–SDC anodes, CeO_2 and Ni-dispersed phases, assuming that after each activation step the anode surface increases at the expense of the dispersed phases,

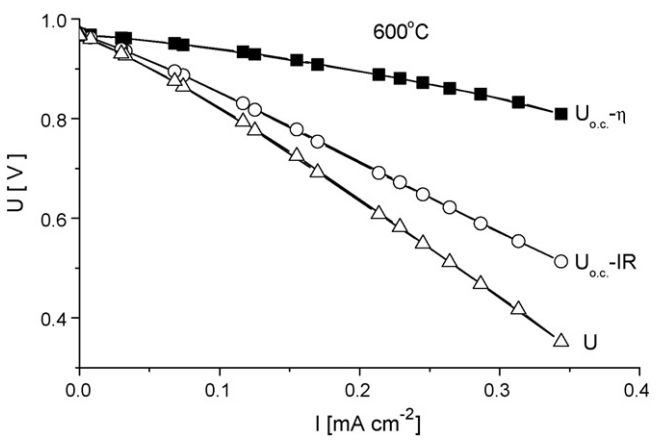

Fig. 5. Contribution of total polarization losses (η) and ohmic polarization losses (IR) to the cell total voltage loss (U) at 600 °C in humidified methane; data obtained for fuel cell II.

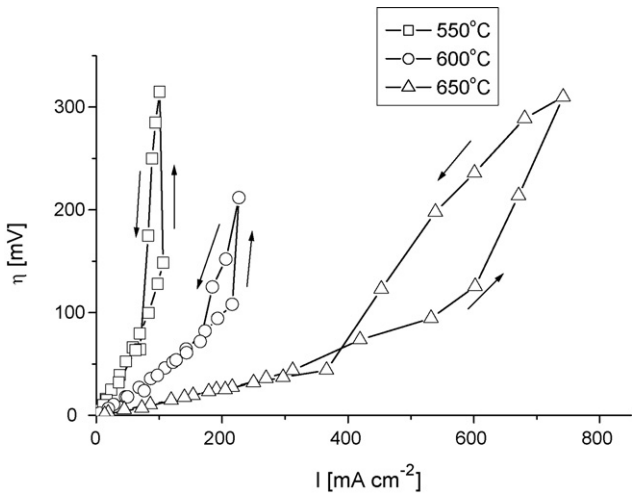

Fig. 6. Anodic polarization curves of a Cu–SDC anode impregnated with CeO_2 and Ni in humidified methane, at 550, 600 and 650 °C; fuel cell II and electrolyte membrane thickness 560 μm.

while the surface of the cermet remained unchanged. The specific surface area of the Cu–SDC bare anode is low, 1.5 $m^2\ g^{-1}$, whereas the specific surface areas of CeO_2 and Ni-dispersed phases are significantly higher, 39.4 and 84.6 $m^2\ g^{-1}$, respectively.

3.2. Fuel cell performance and stability of the new Cu–SDC anode

Fig. 4 shows the characteristic performance of fuel cell I (Cu–SDC anode with CeO_2 and Ni) in: (a) humidified hydrogen and (b) humidified methane, between 500 and 700 °C. The membrane was 250-μm thick. The open circuit voltages (U_{oc}) are high, near 1.05 V on humidified H_2 and 0.9 V in humidified CH_4. As expected the performance in methane is lower than in hydrogen but power densities of ca. 250 mW cm^{-2} were achieved with both fuels, at 600 °C for H_2 and 700 °C for CH_4.

The electrode polarization and membrane ohmic losses were also quantified as function of the current density, and typical data recorded in methane for fuel cell II (Cu–SDC anode with CeO_2 and Ni) is presented in Fig. 5. In all tested fuel cells, and regardless the temperature or fuel, the ohmic loss was the main contribution (ca. 90%) to the total voltage loss. In fact, and as shown in Fig. 6, current densities exceeding 0.4 A cm^{-2} at 650 °C were recorded for 150 mV anodic overvoltage. These data confirm that the new anode performs well with humid methane. Moreover, the fuel cell power density could be increased if a thinner electrolyte membrane would be used. The hystheresis on the anodic polarization curves was due, most probably, to oxidation of nickel near the three-phase boundary at high overvoltage. The nickel oxidation potentials relative to air reference electrode, calculated from thermodynamic values, are −0.825, −0.802, and −0.778 V at 550, 600, and 650 °C, respectively.

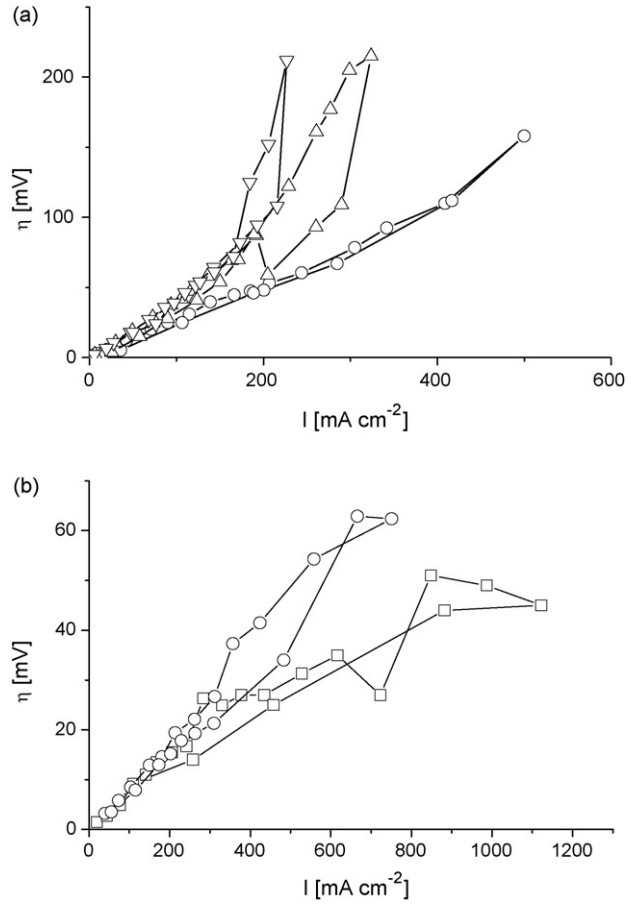

Fig. 7. Anode polarization curves of a Cu–SDC anode impregnated with CeO_2 and Ni at 600 °C in (a) humid methane: (○) first run, (△) second run, (▽) third run; (b) humid hydrogen: (□) before and (○) after operation in humidified methane; fuel cell II and electrolyte membrane thickness 560 μm.

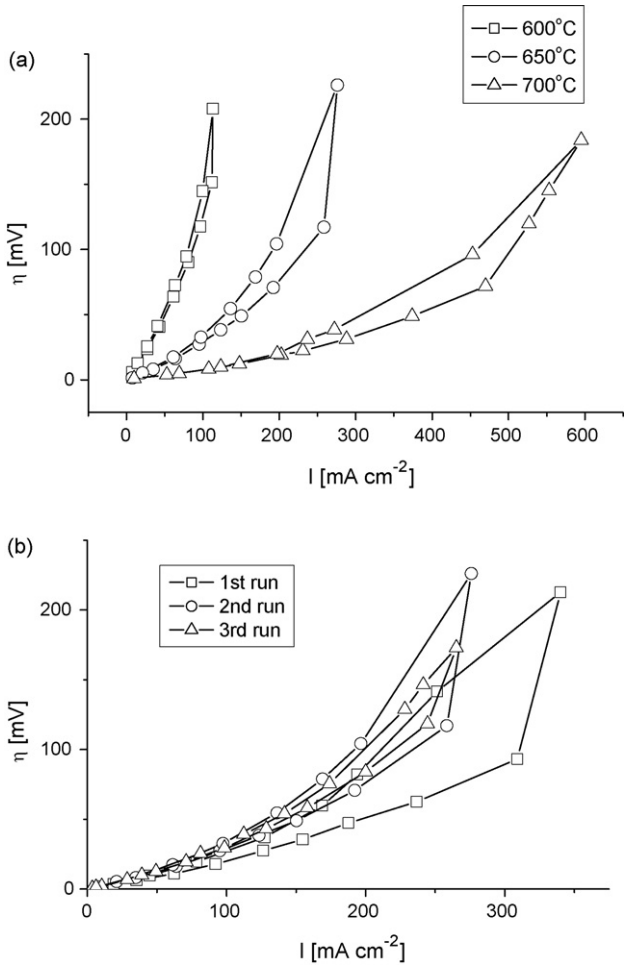

Fig. 8. Anode polarization curves of a Cu–SDC anode impregnated with CeO_2, Ni and MoO_x recorded in humidified methane: (a) between 600 and 700 °C; (b) at 600 °C and after (□) 10 h, (○) 12 h, (△) 19 h operation; fuel cell III and electrolyte membrane thickness 560 μm.

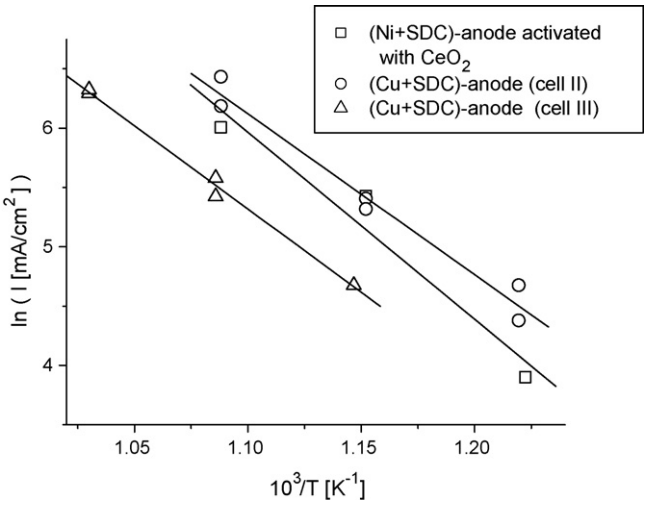

Fig. 9. Temperature dependence of the anodic process rate at $\eta = 150$ mV for Cu–SDC activated anodes of cells II and III and for a Ni–SDC anode; operation in humidified methane.

Nevertheless, the activity and stability of the new anode during operation with methane is still an issue. Fuel cell II was subjected to three short thermal cycles between 500 and 650 °C. The total test time was 24 h from which 11 h were run in methane. Fig. 7 shows the polarization curves recorded at 600 °C: (a) with methane and (b) with hydrogen before and after operation in methane. The anode's activity in methane decreased almost immediately but then it stabilized. The loss in performance was not irreversible since the fuel cell partially recovered when the fuel was switched to hydrogen. A visual inspection of the anode performed after cooling the cell showed that the anode surface was covered with carbon.

Another Cu–SDC anode containing CeO_2 + Ni was further impregnated with MoO_x oxide (fuel cell III, membrane thickness 560 μm) and tested. The aim was trying to improve the fuel cell performance and to prevent carbon deposition as previously reporter by other authors [10]. Fuel cell III operated in both humid hydrogen and methane for a total test period of 64.5 h, 19 h in methane. Fig. 8 presents the anodic polarisation curves recorded for this cell in humidified methane at: (a) different temperatures and (b) 650 °C but in different moments of the cell history.

The performance of fuel cell III was poor in both hydrogen and methane. A visual inspection of the anode performed after cooling the cell also revealed a coat of carbon. Fuel cell III did run more hours in methane than fuel cell II, and a straightforward comparison between both fuel cells is not easy. Too much deposition of MoO_x oxide could have covered partially the electrocatalytic sites and could explain the poor performance of this anode. Finally the MoO_x oxide did not prevent carbon deposition. More work has to be done to clarify these points.

3.3. Electron microscopy of the anode after fuel cell operation

As mentioned above, a visual inspection of the anodes after operation with methane showed the deposition of carbon. Several microphotographs (not shown) of these anodes were also taken. The SDC particles which appeared bright on the new anodes looked now darker as a result of the carbon precipitated on the entire external surface of the anode. However, it is important to mention that the microstructure of the new Cu–SDC anode did not change upon fuel cell operation, which included thermal cycles and fuel switching, and that the copper particles maintained their relative size distribution.

3.4. Temperature dependence of the anodic process rate

Fig. 9 presents temperature dependences of the anodic process rate at $\eta = 150$ mV for Cu–SDC anodes of fuel cells II and III in wet methane. Data for a Ni + SDC anode impregnated with CeO_2 are included for comparison. It is seen that the temperature dependences have nearly equal slopes, and the activation energy is 113 ± 9, 117 ± 6 kJ mol^{-1} for Cu–SDC activated anodes of cells II and III respectively, and 131 ± 30 kJ mol^{-1} for the Ni–SDC anode. This data confirms the high electrocatalytic activity of the new Cu–SDC anode. The activation energy values obtained by us are in the same range of data found in literature for the activation energy of the steam reforming at Ni–YSZ based anodes [16–18].

4. Conclusion

A new copper–cermet anode with samaria-doped ceria electrolyte for solid oxide fuel cells was prepared using ceramic conventional technology from CuO and SDC particles, and further activated with highly dispersed CeO_2 and Ni phases. The new anode performs well in humidified hydrogen and methane in the 500–700 °C temperature range. As expected, the fuel cell performance in humidified methane was lower than in hydrogen; even though, power densities of ca. 250 mW cm^{-2} were recorded at 600 °C in hydrogen and at 700 °C in methane. For operation in methane, current densities higher than 0.4 A cm^{-2} were recorded at 150 mV of anodic overvoltage. Regardless the fuel and temperature, the ohmic loss at the electrolyte membrane was the main contribution to the total voltage loss. The fuel cells suffered an impairment of their activity during the operation with methane. Carbon deposits were found even for the anode having the MoO_x oxide.

References

[1] S. Park, R.J. Gorte, J.M. Vohs, Appl. Catal. A 200 (2000) 55.
[2] J.-H. Koh, Y.-S. Yoo, J.-W. Park, H.C. Lim, Solid State Ionics 149 (2002) 157.
[3] S. Park, R. Cracium, J.M. Vohs, R.J. Gorte, J. Electrochem. Soc. 146 (1999) 3603.
[4] E.P. Murray, T. Tsai, S.A. Barnett, Nature 400 (1999) 649.
[5] C. Lu, W.L. Worrel, R.J. Gorte, J.M. Vohs, J. Electrochem. Soc. 150 (3) (2003) A354–A358.
[6] R.J. Gorte, S. Park, J.M. Vohs, C. Wang, Adv. Mater. 12 (2000) 1465.
[7] S. Jung, C. Lu, H. He, K. Ahn, R.J. Gorte, J.M. Vohs, J. Power Sources 154 (2006) 42.
[8] M.B. Joerger, L.M. Baeurle, L.J. Gluacker, in: Joep Huijmans (Ed.), Fifth European SOFC Forum, Proceedings volume 1, p. 475.
[9] N.Q. Mihn, T. Takahashi, Science and Technology of Ceramic Fuel cells, Elsevier, Amsterdam, The Netherlands, 1995.
[10] A.B. Lopes Correia Tavares, N.M. Bogdanovich, S.M. Beresnev, E. Kh. Kurumchin, Y.A. Dubitsky, A. Zaopo, Solid Oxide Fuel Cell Anode, WO 0506471 A1, Application date 2003.
[11] N.M. Bogdanovich, V.P. Gorelov, V.B. Balakireva, T.A. Dem'yanenko, Russ. J. Electrochem. 41 (2005) 576.
[12] C.M. Finnerty, N.J. Coe, R.H. Cunningham, R.M. Omerod, Catal. Today 46 (1998) 137.
[13] S.P. Jiang, Y.Y. Duan, J.G. Love, J. Electrochem. Soc. 149 (2002) A1157.
[14] Fabricated in IHTE RAS, Inventors certificate No. 1786965.
[15] S. Shinsuke, U. Hiroyuki, W. Masahiro, Solid State Ionics 177 (2006) 359.
[16] S.P. Jiang, S.H. Chem, J. Mater. Sci. 39 (2004) 4405.
[17] E. Achenbach, E. Riensche, J. Power Sources 52 (1994) 283.
[18] V.D. Belyaev, T.I. Politova, O.A. Marina, V.A. Sobyanin, Appl. Catal. A 133 (1995) 47.